

DEVELOPMENT OF A MODEL FOR TRANSIENT SIMULATION AND CONTROL OF A CONTINUOUS STEEL SLAB CASTER

Richard A. Hardin, Kai Liu and Christoph Beckermann

Solidification Laboratory
Department of Mechanical Engineering
University of Iowa
Iowa City, Iowa 52242

Abstract

A two-dimensional heat transfer model for transient simulation and control of a continuous steel slab caster is described. Slab thermal and solidification conditions are computed by the model as a function of time-varying casting speed, secondary spray cooling water flow rates and temperature, slab thickness, steel chemistry, and pouring and ambient temperatures. A solidification model that includes the effects of steel chemistry, cooling rate and microsegregation on the solidification path is incorporated directly into the caster model. Comparisons between measured and predicted liquidus and solidus temperatures are given for two low alloy steels, and show good agreement. Predicted and measured slab surface temperatures recorded on an operating caster are compared with this transient model, and show that the model can predict the temperature response at the slab surface. Results of several simulations are given to demonstrate the effects of changing casting conditions on the slab thermal profile and the solidification end-point. A control methodology suitable for online control of a continuous casting machine is described, and its ability to control the surface temperature profile by dynamically adjusting secondary spray cooling flow rates is demonstrated using the simulator.

Introduction

In order to remain competitive in today's world-wide market for continuously cast steel products, steel producers are finding that it is ever more important to implement process control and to develop a more thorough technological understanding of their casting process. By integrating process control and monitoring into both production and quality control, producers are better able to meet customers' demands for steel of the required quality, quantity, size, grade, and properties at the lowest cost. Computer models used for real-time/on-line prediction and control of continuous steel casters are fundamental tools to accomplish this. Accurate on-line prediction and control of steel solidification and heat transfer allows for more flexibility in caster operation by giving operators the ability to change casting speeds while keeping critical process parameters within required ranges. Such control capability also results in more uniform quality throughout an entire casting sequence from startup to shutdown. Furthermore, due to the unreliability of temperature sensors, and the lack of good sensors for important process parameters such as solidification end-point and liquid pool depth, computer-based control models are often the only available option.

Overview of Previous Work in Transient Caster Modeling and Control

Transient simulation of the continuous casting process is often performed only with the goal of real-time control, and, consequently, such models involve many simplifications. Thermal tracking of the slab cooling history is probably the best tested method of dynamic control of continuous casters, and there are numerous transient heat transfer models presented in the literature used in such control systems. This method of control is well described in the textbook by Irving [1]. The thermal histories of segments of the slab are tracked, and an amount of spray water is applied in order to achieve a prescribed heat transfer coefficient-time relationship. This heat transfer-time relationship is established based on maintaining the temperature profile of the slab that occurs at the design casting speed of the machine. Okuno et al. [2] present a real-time computer model-based secondary spray cooling control system based on tracking the temperatures at planes of the steel slab in real-time and predicting the water flow rate required to maintain set-point surface temperatures at four "control points" along the caster length. Model calculations are performed every 20 seconds. Feedback sensors are used to calibrate the system and assist in recalculating spray water flow rates when the surface temperature is not in agreement with the target temperature. Spitzer et al. [3] present a model which has been used on several casters to control dynamic spray cooling based on tracking slab slices. Online temperature measurements are used along with a solution of the inverse heat conduction problem to adjust the heat transfer coefficients to better control the slab surface temperatures at five set-points. Agreement between model and measured surface temperatures was within 30°C when the online measurements were used to adjust the model's heat transfer coefficients, and within 50°C when no corrections were used.

A dynamic spray cooling model has been developed by Barozzi et al. [4] in which allowable surface temperature ranges at several set-points, shell thickness, and mean exit temperature from the machine are all weighted in controlling both the water flow rates and casting speed. This model uses a combined feed-back and feed-forward technique to control the temperatures at end-zone locations. The feed-back controlled variable is not a measured temperature, but a temperature computed by a dynamic real-time model. A feed-forward loop is applied to calculate the heat flow required to reach the desired set-point from the computed surface temperature, and the water flow rates are adjusted based on this estimation. Computational domains for the solid shell region, and the solidifying mushy region are computed separately. The two regions are

coupled by applying continuity of heat flow across their boundaries, and the equation describing the solidifying region is reduced to an ordinary differential equation by assuming a parabolic temperature profile across the region. Only the heat conduction equation is solved for the solid shell.

A transient heat transfer model for continuous casting of stainless steel is presented by Louhenkilpi et al. [5]. This model uses a non-linear solid fraction versus temperature relationship that is calculated based on steel grade using a separate model prior to running simulations. The model used to compute the temperature-solid fraction relationship and steel properties is presented by Miettinen and Louhenkilpi [6,7]. Spray cooling correlations, which depend upon several variables (spray water flux, slab surface temperature, spray cooling zone number, and steel grade), were determined from a curve fitting procedure based on measured temperatures. Louhenkilpi [6] has also developed an on-line model for solidification end-point prediction, and a dynamic spray cooling control system (CASIM). This control model uses tracking of the residence time of slices of the slab in the caster and look-up tables for solidification end-point versus cooling history (computed from their steady-state model) in order to control the position of the solidification end-point.

Background to the Present Work

The **Dynamic Spray Cooling Simulator (DYSCOS)** computer program presented here, and its real-time control module version were developed during the second and third years of a research program conducted by the Solidification Laboratory at the University of Iowa and IPSCO Inc. DYSCOS simulates transient caster operation with and without dynamic spray cooling control. It is an “offline model”, which includes a high degree of detail but is slower than real-time. Its execution times are slower than real-time by a factor of about four when the code is executed on an Windows NT-based computer with a DEC Alpha 21164 processor. A high degree of detail is used in defining the model’s boundary conditions, including resolving the individual roll contact cooling. This requires that the grid spacing in the axial direction be on the order of 1 mm. By developing a more accurate model first, the tradeoffs between computational speed and model accuracy for coarser, real-time version of the model can be evaluated. This also allows for the testing of control algorithms on both models to study how far the real-time control model might depart from actual processing conditions. By using a multicomponent steel solidification model, the temperature-solid fraction relationship is computed locally for all computational cells in the model. This feature results in the ability to compute changes in the solidification temperature-solid fraction path as the cooling rate varies across the slab thickness. In continuous steel casting the cooling rates from the surface to the centerline can vary by orders of magnitude.

Through a casing conditions input file, operating conditions (such as casting speed, water flow rates, etc.) are input to the model, and the model computes the response of the caster to changing casting conditions. DYSCOS can be run in two modes; a “transient simulation only” mode and a “control” mode. In the “transient simulation only” mode, the casting speed, water flow rates and other operating conditions (pouring temperature, secondary spray water temperature, and ambient temperature) are prescribed to the model and are time-varying. Based on these operating conditions, temperatures and solidification conditions throughout the slab are computed over the time of the simulation. Changes in liquid steel pool depth, solidification end-point, and slab surface temperatures can be observed in response to the input conditions. When used in the “control mode”, DYSCOS computes and stores the flow rates required to maintain a prescribed surface temperature profile on the caster surface along the strand length, in addition to the temperature and solidification data. In both modes of operation, the DYSCOS program

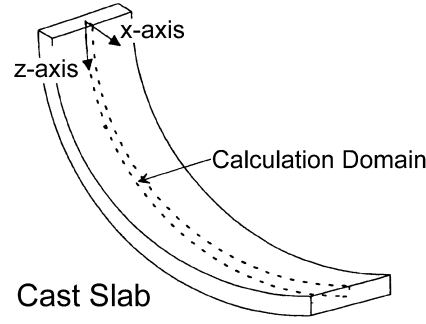


Figure 1: Schematic diagram of the calculation domain in the DYSCOS program.

numerically solves a two-dimensional transient solidification problem at the mid-width position of the slab as shown in Fig. 1.

Model Formulation

Energy Equation

The energy equation describing two-dimensional transient heat transfer and solidification is solved by the DYSCOS program. The calculation domain, as shown in Fig. 1, is a thickness section taken through the mid-width of the slab. This domain extends from the meniscus to an arbitrary distance down to the caster that is user selectable. In order to reduce computation time, symmetry at the centerline of the slab thickness can be assumed. In such a case, only the top surface boundary conditions of the slab are considered. When the model is implemented in its real-time version on the IPSCO machine, sensors will be used only to keep the model in check. Thermal and solutal convection are not considered in this model. The additional energy transport due to convection is approximated through a thermal conductivity enhancement factor that is a function of the solid fraction. Axial conduction is included in this model, but studies with DYSCOS have shown that the axial conduction term does not affect the results appreciably under normal operating conditions. The energy equation describing the above situation is

$$\overline{\rho c_p} \left(\frac{\partial T}{\partial t} + V_{\text{cast}} \frac{\partial T}{\partial z} \right) = \frac{\partial}{\partial x} \left(\overline{k_{\text{eff}}} \frac{\partial T}{\partial x} \right) + \frac{\partial}{\partial z} \left(\overline{k_{\text{eff}}} \frac{\partial T}{\partial z} \right) + S \quad (1)$$

where

$$\overline{\rho c_p} = \epsilon \rho_s c_{ps} + (1 - \epsilon) \rho_l c_{pl}$$

$$\overline{k_{\text{eff}}} = [k_s \epsilon + (1 - \epsilon) k_l] [1 + \beta (1 - \epsilon)^2]$$

$$S = \text{the latent heat source term} = \Delta h \left(\frac{\partial (\epsilon \rho_s)}{\partial t} + V_{\text{cast}} \frac{\partial (\epsilon \rho_s)}{\partial z} \right)$$

and where ρ , c_p , T , t , V_{cast} , z , x , k , ϵ , β , and Δh are the density, specific heat, temperature, time, casting speed, casting direction, thickness direction, thermal conductivity, solid fraction, thermal conductivity enhancement factor, and latent heat, respectively. The subscripts s, l, ref, and eff denote solid, liquid, reference, and effective, respectively. The first term on the left-hand side of Eq. (1) accounts for transient effects, and the energy advected down the slab with the casting speed is taken into account by the second term. The first term on the right side is the x-direction (thickness) conduction term, and the second term is the z-direction (axial) heat conduction term. In continuous steel casting, the axial-direction conduction term is generally much smaller than the x-direction conduction and casting speed advection terms. However, by including this term the model could be applied to continuous casting of higher thermal conductivity materials and should

also remain valid at very low casting speeds. The last term on the right side accounts for the heat released during the solidification process.

Solidification Model

During solidification, the evolution of the temperature and solid fraction is determined according to the cooling conditions of a given cell by coupling the energy equation with the chemical species conservation and back-diffusion model equations for up to fifteen alloying elements whose data are available in the model database. Temperature and the solid fraction in each computational cell are determined through iterations between the energy equation (1), the species conservation equation (2), the microscopic solid-species diffusion equation (3), and equation (4) for the liquidus temperature, T_{mush} ,

$$\epsilon C_s^i + (1 - \epsilon) C_1^i = C_0^i \quad (2)$$

$$\frac{\partial}{\partial t} (\epsilon C_s^i) + V_{\text{cast}} \frac{\partial}{\partial z} (\epsilon C_s^i) = \kappa^i C_1^i \left[\frac{\partial}{\partial t} (\epsilon C_s^i) + V \frac{\partial}{\partial z} (\epsilon C_s^i) \right] + \frac{12 D_s^i}{\lambda_2^2 \epsilon} (\kappa^i C_1^i - C_s^i) \quad (3)$$

$$T_{\text{mush}} = T_{\text{pure}} + \sum_i f(C_1^i) = T_{\text{pure}} + \sum_i m_1^i C_1^i \quad (4)$$

where C , κ , D_s , λ_2 , and m refer to the mass concentration of an element, partition coefficient, mass diffusion coefficient in the solid, secondary dendrite arm spacing, and liquidus slope of the i -th element in the steel, respectively. The “ i ” superscript refers to the i -th chemical element. Equations (1), (2), (3) and (4) are coupled using Newton-Raphson iterations during solidification to determine the solid fraction and temperature according to the local cooling conditions. Equation (3) is based on the assumption of a 1-D, platelike secondary dendrite arm geometry and a parabolic concentration distribution in the solid following the work of Wang and Beckermann [9]. Equation (4) is considered valid provided that the total alloying content is about 6 wt% or less, and the Si content is less than 1 wt%. Since there is no fluid flow and macrosegregation accounted for in this model, the total concentration of any given element is conserved within each computational cell. Finite volume discretization using a TDMA solver and ADI sweeping is used to solve the problem numerically.

This solidification model was tested and verified by imposing a constant cooling rate on a single computational cell, and then comparing the results with liquidus and solidus temperature measurements reported by Howe [10]. Example results of these tests for a steel from [10] are presented in Fig. 2a. For these results the steel composition (wt.%) is 0.11 C, 0.12 Si, 1.25 Mn,

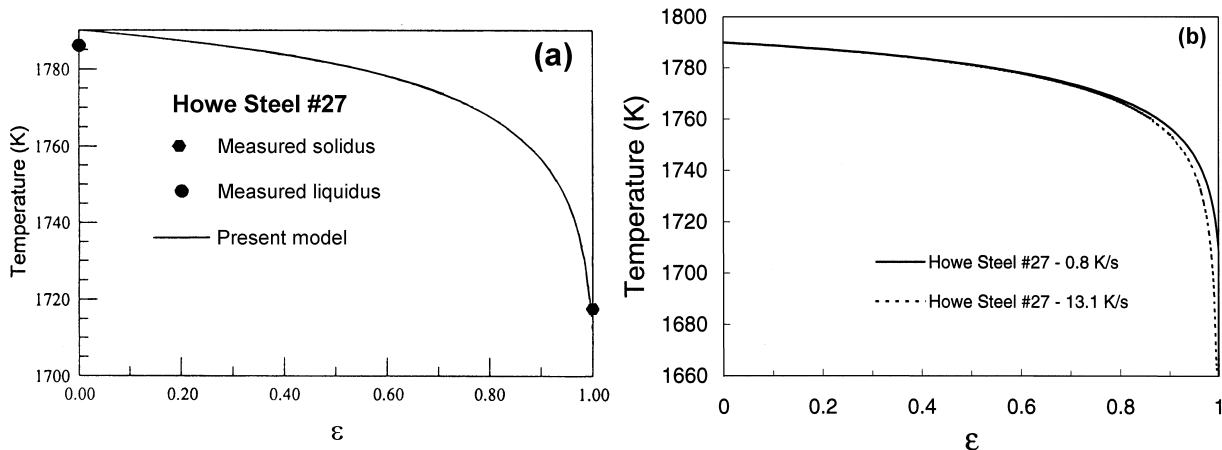


Figure 2: (a) Comparison of measured [10] and predicted solidification ranges for a low alloy steel cooled at 0.8 K/s, (b) cooling rates of 13.1 K/s and 0.8 K/s compared for the same steel.

0.04 P, 0.018 S, 0.06 Cr, 0.07 Mo, 0.03 Ni, and 0.012 N. The model results generally appear to be within 5 °C of the measured liquidus and solidus values for this steel. In Fig. 2b, the effect of cooling rate on solidus temperature is demonstrated, for the cooling rate reported by Howe and a higher cooling rate. The higher cooling rate of 13 K/s would correspond to a point near the slab surface, and for this cooling rate the solidus temperature is markedly lower. The effect of local cooling rate on the solidification path near the end of solidification can be important. For some alloys, this effect alters the solidification path over a wider range of solid fraction (more than just the final 20%) and can be more critical.

Initial and Boundary Conditions, and Properties

As its initial condition, the DYSCOS model assumes that the caster is in operation under steady state conditions. Output from a steady-state model is used to prescribe the initial temperature and solid fraction distributions. A version of this model, Caster-GUI, is discussed in [11]. It was not envisioned that the DYSCOS model would predict the caster startup or shut down processes. However, as the results below will show, the model does a good job of predicting surface temperatures during startup and shutdown of the caster.

Establishing and calibrating proper boundary conditions for a continuous casting machine can be difficult due to the multiple modes of heat transfer involved, and the many variables which are difficult to account for on an actual machine. An average heat flux as a function of dwell time in the mold is used in the DYSCOS mold based on measurements taken from the machines. Thermal radiation is computed over the entire casting surface after the exit of the mold, except at roll contact points. In regions of secondary cooling spray, heat transfer coefficients are used based on the correlation developed by Nozaki et al. [12]. The calibration constants for this relation were determined by an automated iterative process using the steady-state caster model and surface temperature measurements. On IPSCO's Regina caster these constants were statistically determined over three regions of the machine using three weeks worth of data collected online. A single calibration constant was determined for the IPSCO caster in Montpelier, Iowa, based on handheld pyrometer measurements. At the roll contact points, heat transfer coefficients are used which are based on the increase in the background (or local spray) heat transfer coefficient according to measurements in the literature [13,14]. Where there is no spray, natural convection heat transfer coefficients are used for upward facing, down facing and inclined surfaces. The data from Pehlke et al. [15] are used for three categories of low alloy steels (high, medium, and low carbon). More discussion of the properties and the boundary conditions used is given elsewhere [11].

Model Results

At each computed time step, the temperature and solid fraction distribution through the slab are determined for the entire caster. As an example, in Fig. 3a the temperature profile on the surfaces and at the centerline of the slab are shown, and in Fig. 3b the solid fraction distribution for a 15.2 cm thick slab is shown. Note, this is the high-detail model, and in Fig. 3a the cooling at the rolls produces downward temperature spikes. The real-time model averages the contact cooling over the machine segments, which results in a smoother surface temperature profile. Typical run times for this high-detail model can depend on how abruptly the casting conditions change, with faster convergence being achieved for slowly changing conditions. Simulation times can vary between factors of 4 to 20 times real-time, depending on the casting conditions, for a grid of 100 cells through the entire slab thickness by 2500 cells in the casting direction computed on a computer with a 667 MHz DEC Alpha 21164 processor.

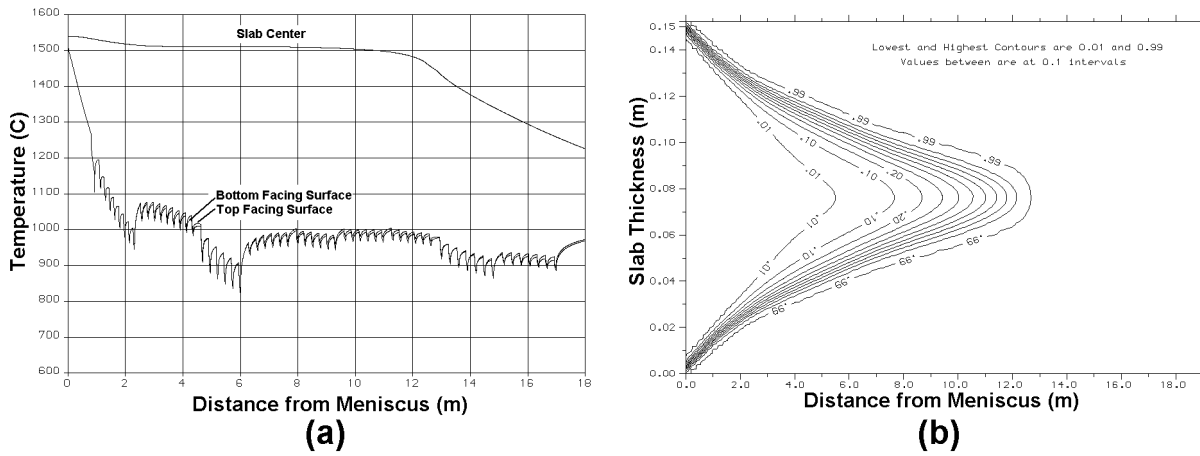


Figure 3: Temperature profile (a) and solid fraction distribution (a) results from high-detail DYSCOS model at an instant in time during a simulation.

Comparisons between measured and predicted transient surface temperature variations at two positions from the meniscus on the slab surface are given in Figures 4 and 5. Simulation conditions are taken from online data acquired during caster operation. The slab thickness being cast in both cases is 10.2 cm. In both figures, the measured surface temperature is initially recorded when the slab first passes beneath the pyrometers as the caster begins operation. In Case 1, shown in Fig. 4, the slab first passes the upper pyrometer (at 9.16 m from meniscus) at 459 s, and the lower pyrometer (at 18.45 m from meniscus) at 795 s. There is good agreement with the measurements for this case even though the model calibration is based on steady-state conditions. At the end of the casting sequence, the model tracks the initial drop in the temperature measurements due to the casting speed drop at about 2600 s. Here note that the model over predicts the initial part of the temperature trough that occurs at 3400s. However, it captures the final temperature recorded at the end of the cast slab quite well. At the lower pyrometer, the model temperature is under predicted by a maximum of 50°C, but the prediction agrees very well with the data trend. The point at which the upper pyrometer measurement drops below the lower measurement is well predicted in the DYSCOS model. For Case 2 (Fig. 5) the startup process is

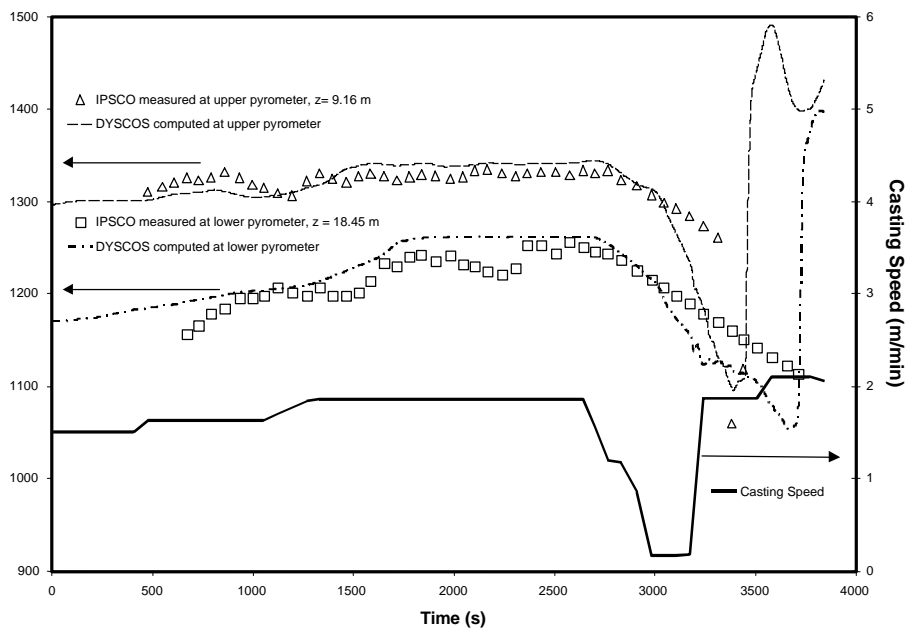


Figure 4: Comparison between measured and predicted slab surface temperatures from high-detail DYSCOS model with the casting speed conditions for 10.2 cm thick slab Case 1.

predicted well by the model at the lower pyrometer position around 670 s. The temperature drop that occurs following the casting speed decrease (at 3463 s) is over predicted again by the model. However, there is a sharp temperature drop here, and, since there is no data beyond 4281 s, it is not known how well the DYSCOS model would have predicted the temperature trough for this case.

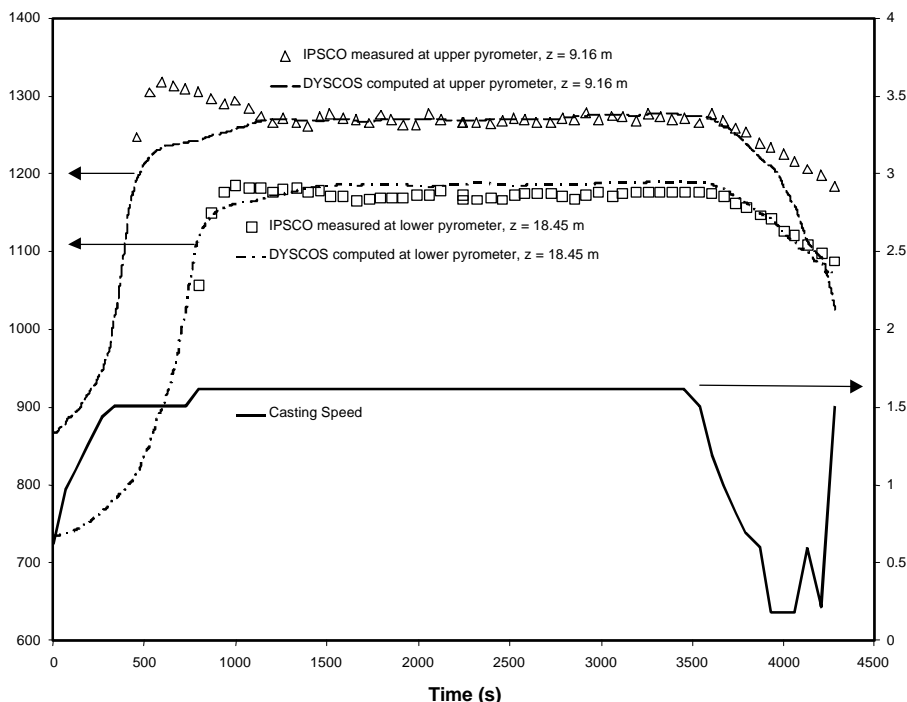


Figure 5: Comparison between measured and predicted slab surface temperatures from high-detail DYSCOS model with the casting speed conditions for 10.2 cm thick slab Case 2.

Results of Studies with and without Spray Cooling Control and the Control Algorithm

Parametric studies were performed to study the relative effects of casting variables on the surface temperatures and solidification conditions for the IPSCO casters in Montpelier, Iowa and Regina, Saskatchewan. Increasing and decreasing casting speed, changing spray cooling water flow rates and temperatures, changing pouring temperature, and even changes in the caster environment temperature were investigated. Changes in the temperature profile and solidification end-point, and the response time required to reach steady-state conditions were among the most critical factors studied since they may affect slab quality. Not surprisingly, casting speed is the most important factor affecting thermal and solidification conditions. The response time of the caster to an increase in casting speed was observed to coincide with the time required for the new conditions to propagate down the caster at the new casting speed. A longer response time than this propagation time is observed for a casting speed decrease. This is due to the additional time required for the mushy zone to attain its new condition, since additional time is required to release the steel's latent heat as the solidifying region shifts to a higher position in the machine. Results of several of these casting speed change studies will be discussed below for cases with and without spray water control.

Using the DYSCOS model, numerous control methodologies were tested for their capability to maintain a prescribed slab surface temperature profile along the caster. Such a control system should maintain temperatures at set-points that are positioned near the end of the spray cooling zones on the machine, with one set-point used to control each secondary spray water loop. To

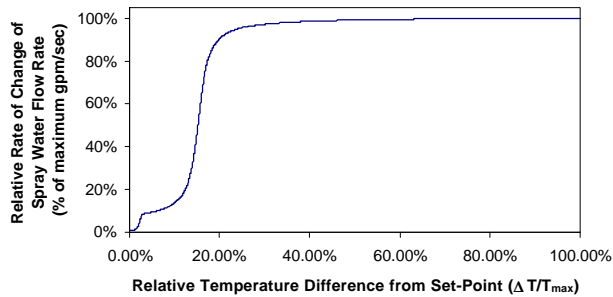


Figure 6: Plot of the control function: rate of water flow rate change (relative to a maximum value) plotted versus absolute relative difference from set-point temperature.

accomplish this, various control-module subprograms were implemented in the transient DYSCOS model. Then the controlled water flow rates from the subprograms are used instead of the prescribed flow rates in the simulations. Traditional feedback and proportional control techniques failed to control the temperatures as well as desired. Based on computational experiments and parametric studies, a control function was established that determines the rate of the adjustment in the water flow rate as a function of the departure of the slab surface temperatures' from the desired set-point value. This difference between the predicted surface temperature and the set-point value is denoted by ΔT . The shape of the function found to give the best performance in terms of stability and response time is shown in Fig. 6.

The flow rate of the zone corresponding to a given set-point is varied as a function of the set-point temperature's difference from the desired set-point temperature. The resulting change in flow rate applied by the control system is also dependent on the set-point monitoring rate in determining the rate of flow rate change. The same function is used to both increase the water flow rate (when the temperature is above the set-point) and decrease the water flow rate (when the temperature is below the set-point). To prevent overshooting, the main cause of fluctuation in the temperature during control, some control logic is used to determine if a change in the water flow rate is to be made. The judgement used is this: when the temperature change is such that it is approaching the set-point temperature, no change will be made in the water flow rate. A change in the water flow rate will be made only if the simulation temperature is moving away from the set-point temperature. In applying this control method to an actual caster, sensors are not required for feedback, but should be strategically used for safety and online calibration of the computer model in implementation as in [4].

In Fig. 7 results from an example case are given where the ability of the control module to maintain the initial temperatures at the control set-points is demonstrated. Here the casting speed is instantaneously stepped from 0.7 m/min to 1.2 m/min at 80 s into the simulation. Note that this is a rigorous test of the control method since casters are not physically capable of such an abrupt speed change. Also, in practice it is not envisioned that precise temperatures at the set-points will not be maintained for all casting speeds; this is merely used here for demonstration purposes. Near the top of the machine (at set-point 1 for instance) the surface temperature is most difficult to control due to the higher temperatures and temperature fluctuations. Also given in this figure are the results of a parametric study on the effect of the same casting speed change with the water flow held constant. Note here that response times for the temperatures to reach steady-state are observed to propagate at the new casting speed down the machine. The water flow rates generated by the control module to maintain the temperatures (for the 0.7 m/min casting speed) are given in Fig. 8. These flow rates demonstrate that maintaining a constant temperature profile for this speed change is impractical, since the flow rates required for some zones are greater than

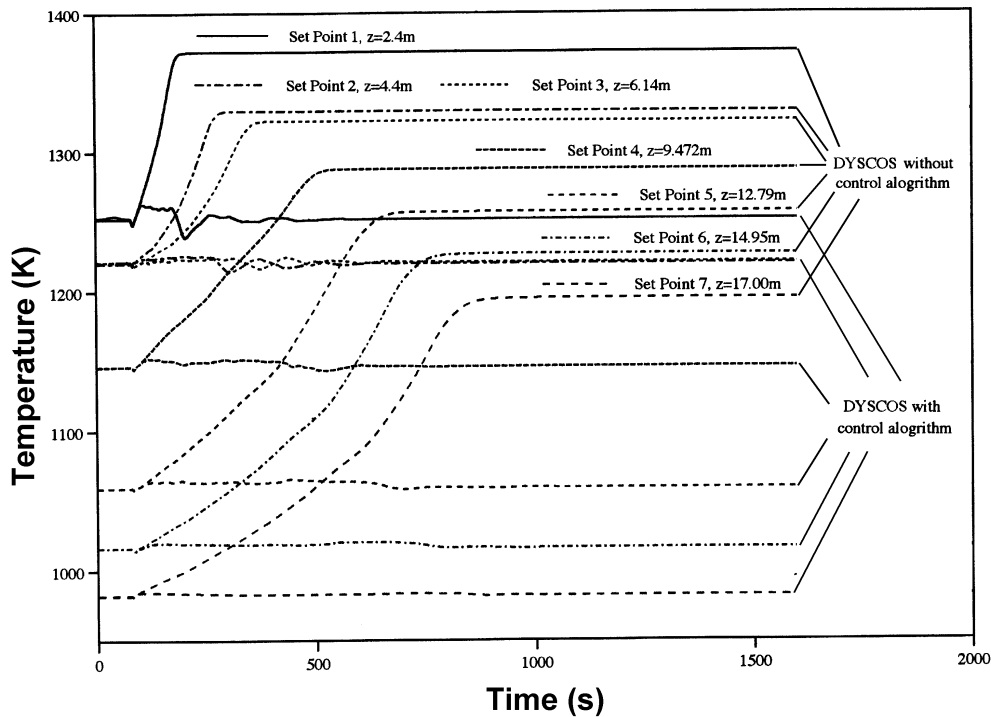


Figure 7: Temperatures at set-points for casting speed change from 0.7 m/min to 1.2 m/min at 80 s with and without using spray cooling control for a 15.2 cm thick slab.

the maximum allowable flow rates for the machine. In the on-line control module, flow limits and allowable surface temperature ranges are added to the control logic.

The solidification conditions inside the slab (depth of liquid pool and solidification end-point) will

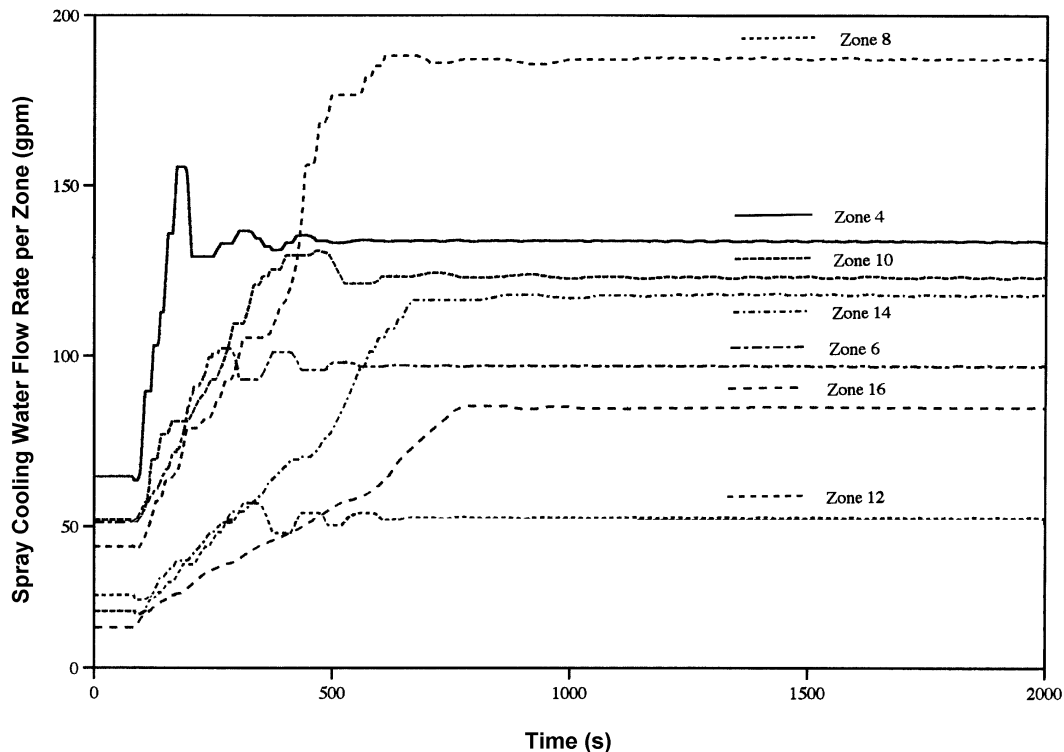


Figure 8: Flow rates generated by DYSCOS control module for case with casting speed change from 0.7 m/min to 1.2 m/min at 80 s for 15.2 cm thick slab.

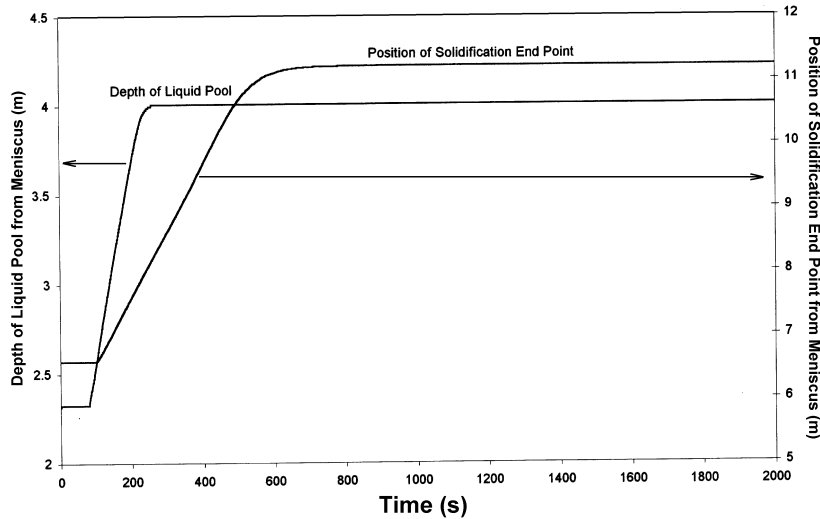


Figure 9: Response of liquid pool depth and solidification end-point to casting speed change from 0.7 m/min to 1.2 m/min at 80 s for 15.2 cm thick slab with control.

change with casting speed even though the surface temperatures are controlled. Depending on the allowable range of these variables, limitations should be placed on the casting speed. In the present control scheme, the casting speed is limited by the maximum and minimum allowable solidification end-point and liquid pool depth. As shown in Fig. 9 for the 0.7 m/min to 1.2 m/min casting speed change with control, the time required for the liquid pool depth and solidification end-point to respond corresponds to the time required for the new conditions to propagate at the new casting speed. The liquid pool settles to its new position approximately 200s after the speed change, and the new position is at about $z = 4$ m. The time required for the new conditions to propagate 4 m into the machine is $(4 \text{ m}) \div (1.2 \text{ m/min}) = 3.33 \text{ min} = 200 \text{ s}$. For the solidification end-point, the response time to the new solidification end-point at 11.25 m is 563 s. This would correspond to 643 s in Fig. 9, which appears to agree quite well with the computed result for solidification end-point response.

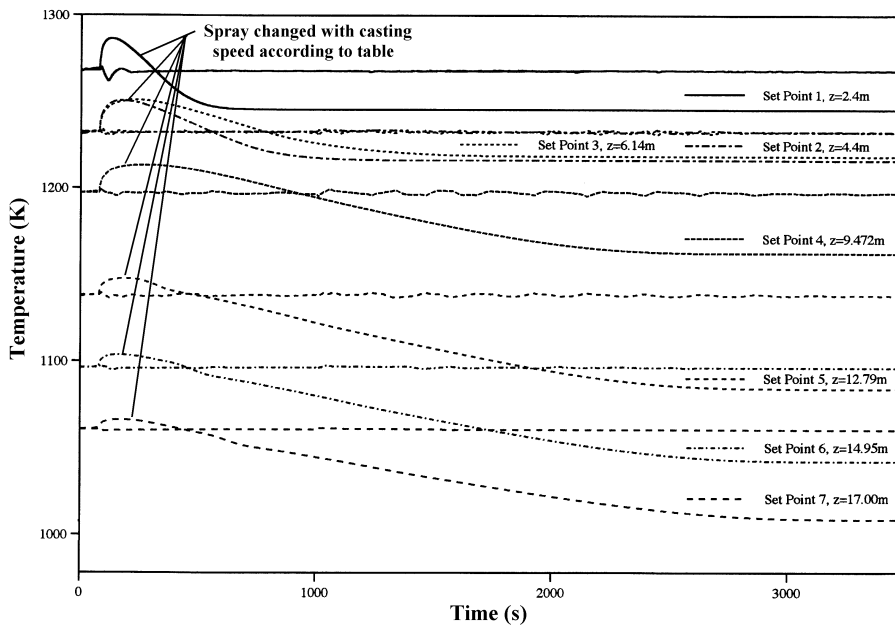


Figure 10: Surface temperatures for casting speed change from 1.0 m/min to 0.8 m/min at 80 s for a 15.2 cm thick slab, flow rates are adjusted according to a prescribed spray table and by the control module (legends for set-point positions are placed above traces for the case where the flow rates are adjusted according to casting speed table).

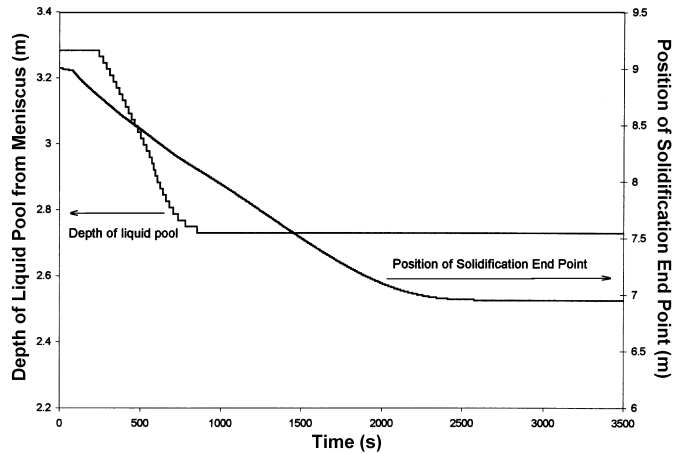


Figure 11: Liquid pool depth and solidification end-point response to casting speed change from 1.0 m/min to 0.8 m/min at 80 s for 15.2 cm thick slab, positions are from meniscus.

Slab surface temperatures at the control set-points are given in Fig. 10 for a decrease in casting speed occurring at 80 s into the simulation. Here the casting speed is changed from 1.0 m/min to 0.8 m/min. For the simulation without control, instead of keeping the flow rates constant, in this case the secondary cooling flows are adjusted according to a flow rate-casting speed lookup table, the method by which the flows are controlled presently for the IPSCO machines. Note the temperature variations that occur when the spray table is used to set the flow rates. For this case, the temperature initially increases as the surface responds quickly to the reduced water flow at the lower speed. As time proceeds, the internal slab temperatures adjust to the new casting conditions and the temperatures decrease well below the initial temperatures. Also given in Fig. 10 are the temperatures at the set-points for the same casting speed change with the control system used to maintain the temperatures at their starting values. Again, the control system works well. The change in liquid pool depth and solidification end-point for this case is given in Fig. 11, where the casting speed spray table is used to control the flow rates. When the casting speed is decreased, it is demonstrated in Fig. 11 that the response times for liquid pool depth and solidification end-point are substantially longer than the time required for the new casting conditions to propagate from the meniscus at the new, lower, casting speed. The response times of the liquid pool depth and the solidification end point to settle to a final steady-state are about 800 s and 2500 s, respectively. The times required for “information” to propagate at the new casting speed (0.8 m/min) from the meniscus to the new liquid pool depth (about 2.73 m) and the to new solid end point (about 6.9 m) are about 205 s and 517 s, respectively. When the casting speed is slowed, the new thermal conditions propagate up the caster and are opposed by the casting speed. Other computational studies have shown that, for the same absolute casting speed change, the solidification conditions require a factor of 4 or 5 times longer to come to equilibrium when the speed is decreased versus a casting speed increase.

Conclusions

Based on the steady-state calibration factors, all comparisons between measured and predicted surface temperatures show that the predictions are on average within $\pm 30^{\circ}\text{C}$ of the measurements for the transient model presented here. The real-time control version of the model requires periodic online calibration, and it is envisioned that a similar dynamic calibration procedure will be implemented in the high-detail DYSCOS model as part of future project work. Parametric studies demonstrate the differences in the thermal and solidification responses of the slab for casting speed increases and decreases. Temperature excursions that occur when a spray cooling table is

used to prescribe the flow rates have been presented. A control method was developed and simulated, which maintains slab surface temperatures within desired ranges. By the results presented here, the DYSCOS model is a valuable and accurate simulator for investigating transients in slab caster operations, and developing control methods. A real-time control module was developed based on numerical experiments performed using DYSCOS, and is currently being installed on the IPSCO Montpelier caster. The real-time online control version of the DYSCOS model solves the same equations on a much coarser mesh with less detailed boundary conditions. The monitoring of the online data and casting conditions requires that separate threads are used in the program to constantly sample the Level 1 caster data and provide updated variables to the online model.

Acknowledgments

The authors gratefully acknowledge their sponsors, IPSCO Inc. for their generous support of this ongoing research program. In particular, the efforts of Dr. Laurie Collins and Mr. Jonathan Dorricott in promoting this collaboration, and the assistance provided by Mr. Atul Kapoor and Mr. Brian Wales in supplying the caster operating and temperature data used to calibrate and test models, are greatly appreciated.

References

1. W.R. Irving, Continuous Casting of Steel, (Institute of Metals, London, 1993).
2. K., Okuno, et al., "Dynamic Spray Cooling Control System for Continuous Casting," Iron and Steel Engineer, 4 (1987), 34-38.
3. K.-H., Spitzer et al., "Mathematical Model for Thermal Tracking and On-line Control in Continuous Casting," ISIJ International, 32 (7) (1992), 848-856.
4. S., Barozzi, P., Fontana, and P., Pragliola, "Computer Control and Optimization of Secondary Cooling During Continuous Casting," Iron and Steel Engineer, 12 (1986), 21-26.
5. S. Louhenkilpi, E. Laitinen, and R. Nienminen, "Real-Time Simulation of Heat Transfer in Continuous Casting," Metall. Trans. B, 24B (1993), 685-693.
6. J. Miettinen, "Calculation of Solidification-Related Thermophysical Properties for Steels", Met. Trans. B, 28B (1997), 281-297.
7. J. Miettinen, and S. Louhenkilpi, "Calculation of Thermophysical Properties of Carbon and Low Alloyed Steels for Modeling of Solidification Processes", Met. Trans. B, vol. 25B (1994), 909-916.
8. S., Louhenkilpi, "Simulation and Control of Heat Transfer in Continuous Casting of Steel," Acta Polytechnica Scandinavica, Chemical Tech. Series No. 230 (1995).
9. C.Y. Wang, and C. Beckermann, Metall. Trans. A, 24A (1993), 2787-2802.
10. A.A. Howe, "Estimation of Liquidus Temperatures for Steels," Ironmaking and Steelmaking, 15 (3) (1988), 134-142.

11. R. Hardin, and C. Beckermann, "Heat Transfer and Solidification Modeling in the Continuous Casting of Multi- Component Steels", HTD-Vol. 347 ASME National Heat Transfer Conference, 9 (1997), 9-20.
12. T. Nozaki, et al., "A Secondary Cooling Pattern for Preventing Surface Cracks of Continuous Casting Slab", Trans. ISIJ, 18 (1978), 330-338.
13. M. El-Bealy, N. Leskinen, and H. Fredriksson, "Simulation of Cooling Conditions in Secondary Cooling Zones in Continuous Casting Process", Ironmaking and Steelmaking, 22 (3) (1995), 246-255.
14. R. York, and H.K. Spitzer, "Heat Transfer in Secondary Cooling Region on Continuous Casting Machines", Solidification Processing 1997: Proceedings of the 4th Decennial International Conference on Solidification Processing, ed. J. Beech and H. Jones (Sheffield, England: University of Sheffield, 1997), 163-165.
15. R.D. Pehlke, A. Jeyarajan, and H. Wada, Summary of Properties for Casting Alloys and Mold Materials, (NSF-MEA-82028, 1982).